Advances in Robotics Research, *Vol. 2, No. 1 (2018) 99-112*
DOI: https://doi.org/10.12989/arr.2018.2.1.099

FPGA-based ARX-Laguerre PIO fault diagnosis in robot manipulator

Farzin Piltan[a] and Jong-Myon Kim*

School of Electrical Engineering, University of Ulsan, Ulsan 680-749, South Korea

(Received January 25, 2018, Revised March 17, 2018, Accepted March 18, 2018)

Abstract. The main contribution of this work is the design of a field programmable gate array (FPGA) based ARX-Laguerre proportional-integral observation (PIO) system for fault detection and identification (FDI) in a multi-input, multi-output (MIMO) nonlinear uncertain dynamical robot manipulators. An ARX-Laguerre method was used in this study to dynamic modeling the robot manipulator in the presence of uncertainty and disturbance. To address the challenges of robustness, fault detection, isolation, and estimation the proposed FPGA-based PI observer was applied to the ARX-Laguerre robot model. The effectiveness and accuracy of FPGA based ARX-Laguerre PIO was tested by first three degrees of the freedom PUMA robot manipulator, yielding 6.3%, 10.73%, and 4.23%, average performance improvement for three types of faults (e.g., actuator fault, sensor faults, and composite fault), respectively.

Keywords: PUMA robot manipulator; FPGA based PI observer; fault diagnosis; ARX method; ARX-Laguerre technique; observation fault diagnosis; PI observation technique

1. Introduction

Industrial robot manipulators are set of links that are connected by diverse of joints. These complex systems are time varying based on wear and tear, multi-input multi-output (MIMO), coupling effect and uncertain which used to replace human workers in many fields such as in industrial or in the manufacturing. Complexities of the tasks and nonlinear parameters in industrial robots caused to have various difficulties for fault diagnosis and tolerant. Therefore, fault detection and isolation (FDI) are necessary to identify faults before impairment the industrial robot. Several types of defects have been defined in industrial robot arms, which are divided into three main categories: actuator faults, plant faults, and sensor faults (Siciliano and Khatib 2016, Ngoc *et al.* 2016).

To fault diagnosis, hardware-based method and functional-based algorithm have been introduced by various researchers (Del Titolo *et al.* 2002). Apart from multiple advantages in hardware-based fault diagnosis, flexibility in design and price are two significant drawbacks. The functionally based fault diagnosis has been introduced to solve these drawbacks (Lafont *et al.*

*Corresponding author, Professor, E-mail: jongmyon.kim@gmail.com
[a]Researcher, E-mail: piltan_f@iranssp.org

http://www.techno-press.org/?journal=arr&subpage=7 ISSN: 2287-4976 (Print), 2287-4984 (Online)

2015, Badihi *et al.* 2017, Wang *et al*. 2016, Khalastch *et al*. 2017, Stavrou *et al*. 2016, Lopez-Estrada *et al*. 2016, Van *et al*. 2016, Anh *et al*. 2012, Alavandar *et al*. 2008, Jami'in *et al*. 2016, Hartmann *et al*. 2015). Model-free fault diagnosis (Lafont *et al*. 2015, Badihi *et al*. 2017), Knowledgebase fault diagnosis (Wang *et al*. 2016, Khalastch *et al*. 2017), and model-based fault diagnosis (Stavrou *et al*. 2016, Lopez-Estrada *et al*. 2016, Van *et al*. 2016), are the main sub-parts of functionally based fault diagnosis. Observer techniques, system identification, and system estimation algorithms are the main techniques based on the model reference fault diagnosis.

System modeling based on the identification algorithm is a powerful tool for fault diagnosis that has acknowledged by various specialists in the field (Forrai and Alexandru 2017) as well (Xia *et al*. 2016). Linear and nonlinear system identification has been introduced to model and estimates the systems based on input and output data and regression method. The primary key to system identifications based on the linear and nonlinear processes are definition of a function to estimate the output based on input data to reduce the cost function. However, linear estimation techniques are widely used in many applications, but it has drawbacks to modeling the noisy and highly nonlinear systems. Nonlinear intelligent system identification and mathematical techniques for system identification are two main methods to improve the performance in the linear techniques for system identification (Anh *et al*. 2012, Alavandar *et al*. 2008, Jami'in *et al*. 2016, Hartmann *et al*. 2015). Regarding (Bouzrara *et al*. 2012, 2013), the mathematical system identification algorithm based on the Laguerre method has been used to reduce the nonlinear parameters in system modeling. The performance of ARX method can be improved by the ARX-Laguerre method.

Estimate the internal state based on the measurements of the real input and output system is defined as state observer. The state observer methods are divided into two main groups, linear-based observer, and nonlinear based observer. Proportional and integral (PI) observers (Busawon and Kabore 2001, Gao 2008, Zhang *et al*. 2013) and proportional multiple-integral (PMI) observers (Gao and Ho 2004, Koenig 2005, Gao *et al*. 2007) are two types of the linear-based observer and adaptive based observer (Zhang and Besancon 2008, Zhang *et al*. 2008, Gholizadeh and Salmasi 2014, Alwi and Edwards 2014), sliding mode observers (Van *et al*. 2016, Alwi and Edwards 2014, Han *et al*. 2014), and descriptor observers (Gao and Wang 2006, Gao *et al*. 2008) are defined as the nonlinear based observer. These methods are usually utilized for fault estimation/reconstruction. The hybrid technique based on the integral observer, sliding observers, and adaptive observers are analyzed by Zhang *et al*. (2013). In Gao *et al*. (2008), to estimate the faults in engine PI observer and descriptor observer techniques are integrated. Field programmable gate array (FPGA) has parallel architecture, and high-speed processing causes it. FPGA-based fault diagnosis has been widely used in industries such as power converters (Jamshidpour *et al*. 2015), bearing (Kang *et al*. 2015) and motor drive (Salehifar *et al*. 2015). In this research, the proposed FPGA-based ARX-Laguerre PI observation method is used to modify the traditional PI observer by applying an ARX-Laguerre technique to estimate the output without a state estimation and FPGA system to improve the rate of speed. The first objective of this research is modeling the robot manipulator and fault detection based on the ARX-Laguerre method. The second objective is designing a PIO method and applied to the ARX-Laguerre technique to improve the performance of input/output fault diagnosis in robot manipulator. The third objective is to develop FPGA-based ARX-Laguerre PIO for fault diagnosis for the robot manipulator. This paper has the following sections. The second section outlines the problem statements. The ARX-Laguerre method for system modeling is presented in the third section. The FPGA-based PI observer is designed and analyzed for fault identification, and estimation is existing in the fourth section. In the fifth section, we can be examined the fault detection, estimation, and identification of the proposed method. In the final part, we provide conclusions.

2. Problem statements and observer objectives

PUMA robot manipulator is serial links, six degrees of freedom, and the dynamic of this system is highly nonlinear, time-varying, MIMO, uncertain and it has substantial coupling effects between joints. Therefore, mathematical modeling in this system in the presence of uncertainty and faults is complicated. The dynamic formulation of robot manipulator in the presence of uncertainty and faults is considered by the following formulations (Siciliano and Khatib 2016)

$$\tau = I(q)[\ddot{q}] + V(q,\dot{q}) + G(q) + F(\dot{q}) + \tau_d + \eta(t-t_f), \tag{1}$$

where $\tau, \tau_d, I(q), V(q,\dot{q}), G(q), F(\dot{q}), \eta(t-t_f), q, \dot{q}$ and $\ddot{q}$ are $n\times 1$ torque vector, $n\times 1$ disturbance of load vector, time variant $n\times n$ inertial matrix, time variant nonlinearity term matrix, time variant $n\times 1$ gravity vector, friction matrix, faults (actuator, plant, sensor), position vector, velocity vector, and acceleration vector, respectively. The time variant nonlinearity term matrix is defined as follows

$$V(q,\dot{q}) = B(q)[\dot{q} \quad \dot{q}] + C(q)[\dot{q}]^2 \tag{2}$$

where $B(q)$ and $C(q)$ are time variant $n\times\frac{n\times(n-1)}{2}$ Coriolis force matrix, and time variant $n\times n$ centrifugal matrix, respectively.

$$\tau = I(q)[\ddot{q}] + B(q)[\dot{q} \quad \dot{q}] + C(q)[\dot{q}]^2 + G(q) + F(\dot{q}) + \tau_d + \eta(t-t_f), \tag{3}$$

Based on Eqs. (1)-(3), the dynamic formulation of robot manipulator is written as follows

$$\iint [\ddot{q}] = \iint I(q)^{-1} \times (\tau - H(q,\dot{q})) + \Phi(q,\dot{q},t), \tag{4}$$

$$H(q,\dot{q}) = B(q)[\dot{q} \quad \dot{q}] + C(q)[\dot{q}]^2 + G(q) \tag{5}$$

$$\Phi(q,\dot{q},t) = I^{-1}(q)(-F(\dot{q}) - \tau_d - \eta(t-t_f)) \tag{6}$$

In healthy condition ($\eta(t-t_f)=0$), the uncertainty is bounded as follows

$$\left\| I^{-1}(q)(-F(\dot{q}) - \tau_d - 0) \right\| = \Phi_0(q,\dot{q},t) \le \Gamma \tag{7}$$

where Γ is constant. In faulty condition ($\eta(t-t_f)\neq 0$), $\Phi(q,\dot{q},t)$ is bounded as follows

$$\left\| I^{-1}(q)(-F(\dot{q}) - \tau_d - \eta(t-t_f)) \right\| = \Phi(q,\dot{q},t) >> \Gamma \tag{8}$$

To solve the challenge of mathematical formulation and fault detection ARX-Laguerre methodology is recommended.

$$\begin{cases} X(k) = [AX(k-1) + b_y y(k-1) + b_u u(k-1)] + \Phi(k-1) + \eta_a(k-1) \\ Y(k) = (K)^T X(k) + \eta_s(k-1) \end{cases} \tag{9}$$

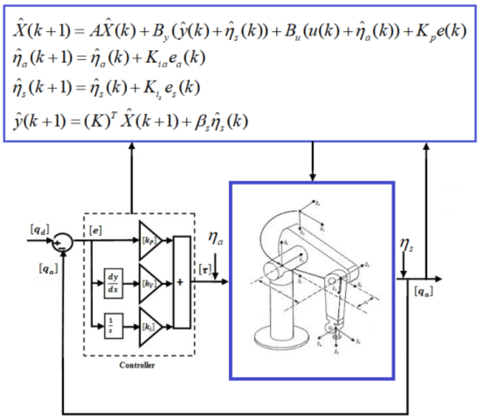

Fig. 1 Robot manipulator PI observer for fault diagnosis

where $X(k), y(k), u(k), \Phi(k), \eta_a(k), \eta_s(k)$ are the system state, measured output, control input, uncertainty and disturbance, actuator fault and sensor fault, and A, b_y, b_u are known coefficient matrices respectively. The second challenge is fault diagnosis (sensor fault and actuator fault) of robot manipulator in the presence of uncertainty and external disturbance. The PI observation technique is applied to Eq. (9) to localization the input/output faults as follows

$$r(k) = \left[X_{output}^T(k) \quad X_{input}^T(k)\right]^T - \left[\hat{X}_{output}^T(k) \quad \hat{X}_{input}^T(k)\right]^T \tag{10}$$

where $r(k)$ is the residual signal for fault detection and isolation. The PI observation technique is used to estimate the state and faults in robot manipulator. The third challenge is the FPGA-based PI observer for fault diagnosis. The block diagram of system observation technique for fault diagnosis is illustrated in Fig. 1. The PI observation technique objectives for robot manipulator in the presence of uncertainty, external disturbance and faults are fault detection and isolation based on the following steps. The first step is detected the normal condition based on the following algorithm

$$\begin{cases} \bar{x}_{N(i),y}(k) - \hat{x}_{N,\hat{y}}(k) \le \Gamma_{out} \\ \bar{x}_{N(i),u}(k) - \hat{x}_{N(i),u}(k) \le \Gamma_{in} \end{cases} \tag{11}$$

The second step is detecting the actuator fault based on the following method

$$\begin{cases} \bar{x}_{N(i),y}(k) - \hat{x}_{N,\hat{y}}(k) \le \Gamma_{out} \\ \bar{x}_{N(i),u+\eta_a}(k) - \hat{x}_{N(i),u}(k) >> \Gamma_{in} \end{cases} \tag{12}$$

To detect and isolated the sensor fault in robot manipulator the following technique is recommended

$$\begin{cases} \bar{x}_{N(i),y+\eta_s}(k) - \hat{x}_{N,\hat{y}}(k) >> \Gamma_{out} \\ \bar{x}_{N(i),u}(k) - \hat{x}_{N(i),u}(k) \le \Gamma_{in} \end{cases} \tag{13}$$

In the last step to detect and isolate the input and output fault based on PI observation technique, following technique is recommended

$$\begin{cases} \bar{x}_{N(i),y+\eta_s}(k) - \hat{x}_{N,\hat{y}}(k) >> \Gamma_{out} \\ \bar{x}_{N(i),u+\eta_a}(k) - \hat{x}_{N(i),u}(k) >> \Gamma_{in} \end{cases} \tag{14}$$

where (Γ_{out}, Γ_{in}) is bounded on uncertainty.

3. ARX-Laguerre PUMA robot manipulator modeling

Regarding Eq. (9), the dynamic modeling of robot manipulator based on the ARX-Laguerre method in the presence of uncertainty, external disturbance, and faults has been presented as follows (Bouzrara *et al*. 2012, 2013)

$$\begin{aligned} & y(k) = \sum_{0}^{N_a-1} K_{(n,a)} x_{(n,y)}(k) + \sum_{0}^{N_b-1} K_{(n,b)} x_{(n,u)}(k) \\ & X(k) = \left[x_{(n,u)}(k) \quad x_{(n,y)}(k) \right] \\ & x_{(n,y)}(k) = L_n^a(k, \xi_a) * y(k) \\ & x_{(n,u)}(k) = L_n^b(k, \xi_b) * u(k) \end{aligned} \tag{15}$$

where $y(k), u(k), (K_{n,a}, K_{n,b}, N_a, N_b), x_{(n,y)}(k), x_{(n,u)}(k), (L_n^a(k,\xi_a), L_n^b(k,\xi_b))$ are the system state output, system state input, Fourier coefficients, output signal filter, input signal filter, and Laguerre-based orthonormal functions, respectively. Based on Eqs. (9) and (15), the state space dynamic modeling of robot manipulator based on the ARX-Laguerre in the presence of the external disturbance, uncertainty and (actuator and sensor) faults are obtained by the following formulation

$$\begin{cases} \bar{X}(k) = [A\bar{X}(k-1) + b_y \bar{y}(k-1) + b_u u(k-1)] + \bar{\Phi}(k-1) + \bar{\eta}_a(k-1) \\ \bar{Y}(k) = (K)^T \bar{X}(k) + \bar{\eta}_s(k-1) \end{cases} \tag{16}$$

After modeling the robot manipulator based on the ARX-Laguerre method, the fault can be detected by defined the input/output residual signal.

$$\begin{bmatrix} r_{out} \\ r_{in} \end{bmatrix} = \begin{bmatrix} x_{N(i),y}(k) - \bar{x}_{N,\hat{y}}(k) \\ x_{N(i),u}(k) - \bar{x}_{N(i),u}(k) \end{bmatrix} \tag{17}$$

Based on Eq. (17), if $\begin{cases} \eta_s \neq 0 \\ \eta_a \neq 0 \end{cases}$, the input/output faults are detected in robot manipulator based on the following formulation

$$\begin{cases} (\eta_s \neq 0 / \eta_a \neq 0) \to (y(k) - \bar{y}(k) >> \Gamma) \,\&\, (X(k) - \bar{X}(k)) >> \Gamma_{in} / \Gamma_{out} \\ (\eta_s = 0 / \eta_a = 0) \to (y(k) - \bar{y}(k) \leq \Gamma) \,\&\, (X(k) - \bar{X}(k)) \leq \Gamma_{in} / \Gamma_{out} \end{cases} \tag{18}$$

Therefore, normal and abnormal robot manipulators can be identified based on Eqs. (17) and (18). In order to verify the performance of ARX-Laguerre method to modeling, this method is tested and compare with the conventional ARX method. The comparison error performance between proposed method and ARX method is depicted in Fig. 2. Regarding to this figure, the error performance in proposed method is better than ARX technique. The rate of RMS error in

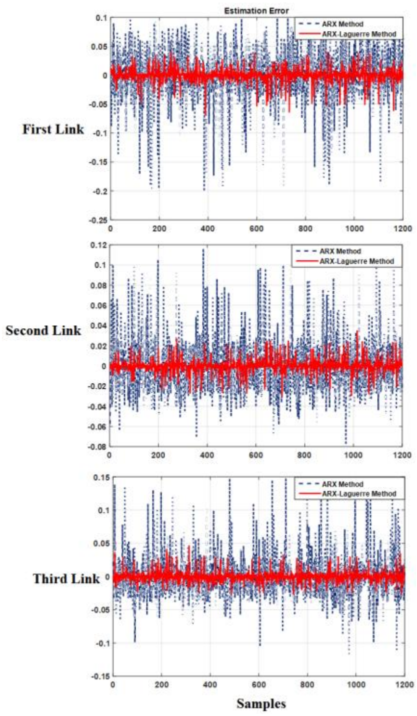

Fig. 2 Estimation error for first, second and third joint: ARX-Laguerre method and ARX method

proposed error for first, second and third joints are 0.04°, 0.02°, and 0.04°, and for ARX techniques are 0.15°, 0.1°, and 0.13°, respectively.

4. FPGA- based PI observer fault diagnosis in robot manipulator

The proposed ARX-Laguerre PI observations technique is recommended for estimating and identifying the actuator and sensor faults in the robot manipulator. In the first step, the formulation of ARX-PI observer for robot manipulator is introduced in Eq. (19) and in the next step the formulation of the ARX-Laguerre PI observation technique for fault diagnosis in robot manipulator is detailed in Eq. (20). According to Eqs. (19) and (20), the actuator and sensor faults are estimated based on an integral part of PI observation technique. To fault diagnosis in robot manipulator based on PI observation technique, we can define four different cases.

Case A: In healthy condition of robot manipulator, if $\eta_a = 0, \eta_s = 0$, the fault diagnosis algorithm can be calculated in Eq. (21).

Case B: If robot manipulator has actuator fault ($\eta_a \neq 0, \eta_s = 0$), based on PI observation technique the fault diagnosis algorithm is obtained in Eq. (22).

$$\begin{cases} \hat{X}(k) = [A\hat{X}(k-1) + b_u u(k-1)] + \hat{\Phi}(k-1) + \hat{\eta}_a(k-1) + \\ K_{p_a}(X(k-1) - \hat{X}(k-1)) + K_{p_s}(X(k-1) - \hat{X}(k-1)) \\ \hat{Y}(k) = (K)^T \hat{X}(k) + \hat{\eta}_s(k-1) \\ \hat{\eta}_a(k) = \hat{\eta}_a(k-1) + K_{ia}(X(k-1) - \hat{X}(k-1)) \\ \hat{\eta}_s(k) = \hat{\eta}_s(k-1) + K_{is}(X(k-1) - \hat{X}(k-1)) \end{cases} \tag{19}$$

$$\begin{cases} \hat{X}(k) = [A\hat{X}(k-1) + b_y\hat{y}(k-1) + b_u u(k-1)] + \hat{\Phi}(k-1) + \hat{\eta}_a(k-1) + \\ K_{p_a}(\bar{x}_{N(i),u}(k-1) - \hat{x}_{N(i),u}(k-1)) + K_{p_s}(\bar{x}_{N(i),y}(k-1) - \hat{x}_{N(i),y}(k-1)) \\ \hat{Y}(k) = (K)^T\hat{X}(k) + \hat{\eta}_s(k-1) \\ \hat{\eta}_a(k) = \hat{\eta}_a(k-1) + K_{ia}(\bar{x}_{N(i),u}(k-1) - \hat{x}_{N(i),u}(k-1)) \\ \hat{\eta}_s(k) = \hat{\eta}_s(k-1) + K_{is}(\bar{x}_{N(i),y}(k-1) - \hat{x}_{N(i),y}(k-1)) \end{cases} \tag{20}$$

$$\begin{aligned} &(\bar{y}(k) - \hat{y}(k) \le \Gamma)\,\&\,(\bar{X}(k) - \hat{X}(k)) \le \Gamma \Rightarrow \left[\bar{X}_1^T(k) \quad \bar{X}_2^T(k)\right]^T - \\ &\left[\hat{X}_1^T(k) \quad \hat{X}_2^T(k)\right]^T \le \Gamma \Rightarrow \begin{cases} \bar{x}_{N(i),y}(k) - \hat{x}_{N,\hat{y}}(k) \le \Gamma_{out} \\ \bar{x}_{N(i),u}(k) - \hat{x}_{N(i),u}(k) \le \Gamma_{in} \end{cases} \end{aligned} \tag{21}$$

$$\begin{aligned} &(\bar{y}(k) - \hat{y}(k) \le \Gamma)\,\&\,(\bar{X}(k) - \hat{X}(k)) > \Gamma \Rightarrow \left[\bar{X}_1^T(k) \quad \bar{X}_{2+\eta_a}^T(k)\right]^T - \\ &\left[\hat{X}_1^T(k) \quad \hat{X}_2^T(k)\right]^T > \Gamma \Rightarrow \begin{cases} \bar{x}_{N(i),y}(k) - \hat{x}_{N,\hat{y}}(k) \le \Gamma_{out} \\ \bar{x}_{N(i),u+\eta_a}(k) - \hat{x}_{N(i),u}(k) >> \Gamma_{in} \end{cases} \end{aligned} \tag{22}$$

Case C: In sensor faulty condition ($\eta_a = 0, \eta_s \ne 0$), the PI observation algorithm for fault diagnosis is calculated by the following formulation.

$$\begin{aligned} &(\bar{y}(k) - \hat{y}(k) >> \Gamma)\,\&\,(\bar{X}(k) - \hat{X}(k)) > \Gamma \Rightarrow \left[\bar{X}_{1+\eta_s}^T(k) \quad \bar{X}_2^T(k)\right]^T - \\ &\left[\hat{X}_1^T(k) \quad \hat{X}_2^T(k)\right]^T > \Gamma \Rightarrow \begin{cases} \bar{x}_{N(i),y+\eta_s}(k) - \hat{x}_{N,\hat{y}}(k) >> \Gamma_{out} \\ \bar{x}_{N(i),u}(k) - \hat{x}_{N(i),u}(k) \le \Gamma_{in} \end{cases} \end{aligned} \tag{23}$$

Case D: Finally, in input and output faulty condition ($\eta_a \ne 0, \eta_s \ne 0$), the PI observation algorithm for fault diagnosis is calculated by the following formulation.

$$\begin{aligned} &(\bar{y}(k) - \hat{y}(k) >> \Gamma)\,\&\,(\bar{X}(k) - \hat{X}(k)) >> \Gamma \Rightarrow \left[\bar{X}_{1+\eta_s}^T(k) \quad \bar{X}_{2+\eta_a}^T(k)\right]^T - \\ &\left[\hat{X}_1^T(k) \quad \hat{X}_2^T(k)\right]^T >> \Gamma \Rightarrow \begin{cases} \bar{x}_{N(i),y+\eta_s}(k) - \hat{x}_{N,\hat{y}}(k) >> \Gamma_{out} \\ \bar{x}_{N(i),u+\eta_a}(k) - \hat{x}_{N(i),u}(k) >> \Gamma_{in} \end{cases} \end{aligned} \tag{24}$$

Figs. 3-5 illustrate the block diagram of FPGA-based proposed method, FPGA- based fault estimation algorithm and FPGA-based state condition algorithm and state algorithm.

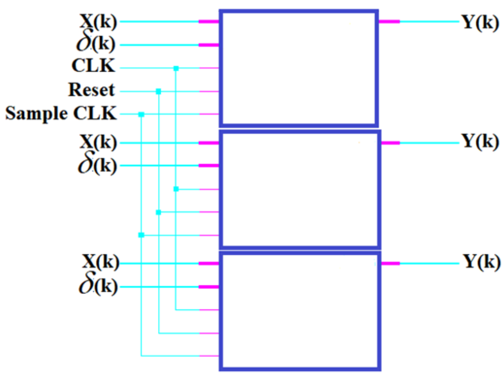

Fig. 3 Block diagram of FPGA-based PI observer ARX-Laguerre

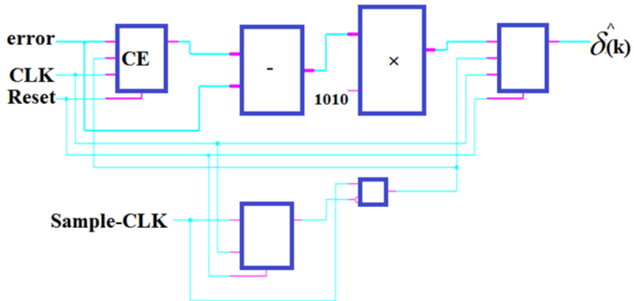

Fig. 4 Fault estimation algorithm

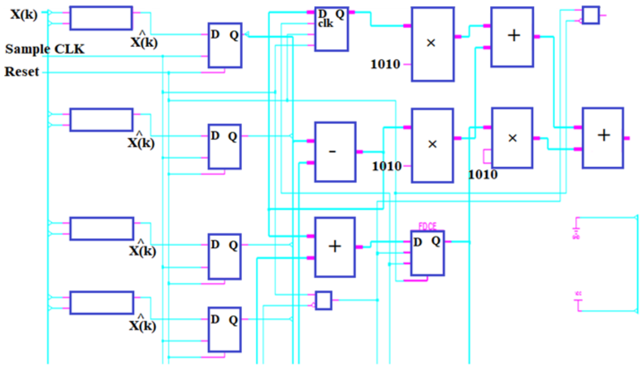

Fig. 5 State condition algorithm

5. Results and discussion

Case Study: To test and analyze FPGA-based ARX-Laguerre PI observation method for actuator and sensor faults diagnosis in a robot manipulator, a PUMA robot manipulator was selected. The residual signal for the effect of the actuator and the effect of the sensor is calculated as follows

$$\begin{bmatrix} r_{out} \\ r_{in} \end{bmatrix} = \begin{bmatrix} x_{N(i),y}(k) - \bar{x}_{N,\hat{y}}(k) \\ x_{N(i),u}(k) - \bar{x}_{N(i),u}(k) \end{bmatrix} = \begin{bmatrix} 20(N.m) \\ 0.02(Rad) \end{bmatrix} \tag{25}$$

These two threshold values are used for fault detection and identification. The actuator fault in the first three links is defined based on the following functions

$$\eta_a(N.m) = \begin{cases} 45, t \geq 0.1(s) \\ 0, otherwise \end{cases} \tag{26}$$

The sensor fault for robot manipulator is defined based one the following function

$$\eta_s(Rad) = \begin{cases} 0.8, t \geq 1(s) \\ 0, otherwise \end{cases} \tag{27}$$

Fig. 6 demonstrates the input and output results robot manipulator in healthy condition for first three links. Regarding Fig. 6, the actuator and sensor fault detector is zero. Fig. 7 illustrates the actuator fault diagnosis in PUMA robot manipulator. Regarding Fig. 7 and Eq. (26), in PI observation technique the time of fault detection and identification for actuator fault in first, second, and third links are 0.114(sec), 0.2706(sec), 0.3385(sec), respectively. Fig. 8 demonstrates the PI observer fault diagnosis to detect and identification of sensor fault for PUMA robot manipulator.

Based on Eq. (27), sensor fault applied to robot manipulator at $\eta_s(Rad)=\begin{cases}0.8, t\geq 1(S)\\ 0, t<1(S)\end{cases}$. Regarding to Fig. 8, the detection and identification time for first, second and third links are 1.166(sec), 1.322(sec), 1.504(sec), respectively.

Based on Fig. 9, the detection and identification time for composed (actuator+sensor) fault diagnosis for first three degrees of PUMA robot manipulator are 0.2438(sec), 0.32227(sec), 0.4539(sec), 1.442(sec),1.638(sec), 1.822(sec), respectively. According to the results from Figs. 6-9, we can see that our proposed PI observation technique is highly useful to detect actuator and sensor fault states. To further validate our model and fault diagnosis technique, we calculate the diagnostic delay time for each failure for first three links of PUMA robot manipulator in proposed ARX-Laguerre PI observer method and ARX PI observer technique. Tables 1-5 present the diagnosis delay time in FPGA-based ARX-Laguerre PIO and FPGA-based ARX PIO for first three joints of PUMA robot manipulator.

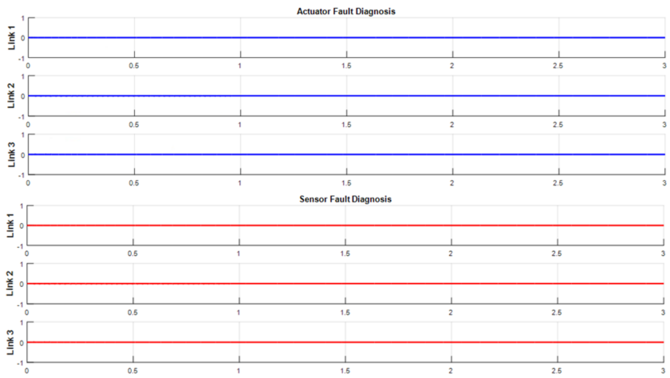

Fig. 6 Fault diagnosis in first three links of robot manipulator in normal

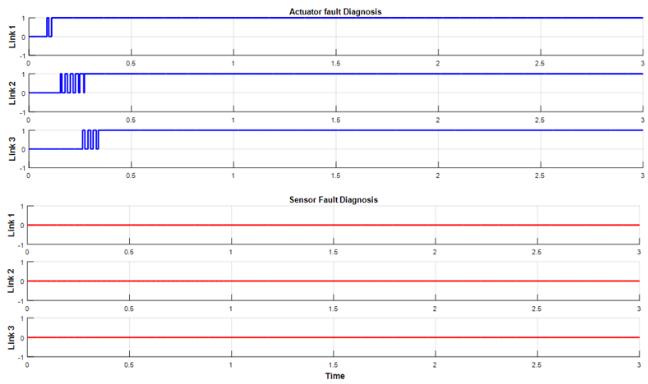

Fig. 7 Fault diagnosis in first three links of robot manipulator with actuator faulty condition

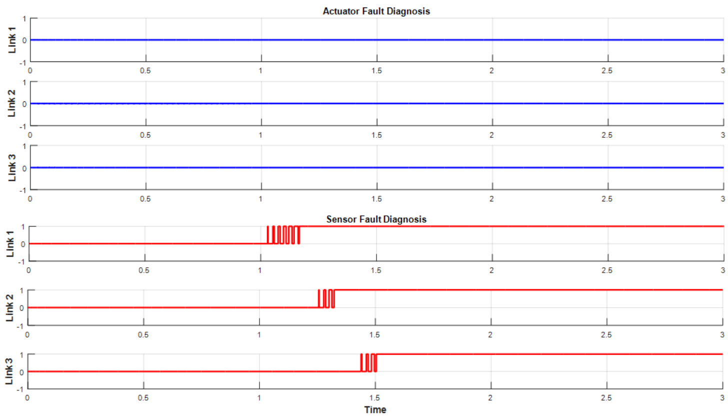

Fig. 8 Fault diagnosis in first three links of robot manipulator with sensor faulty condition

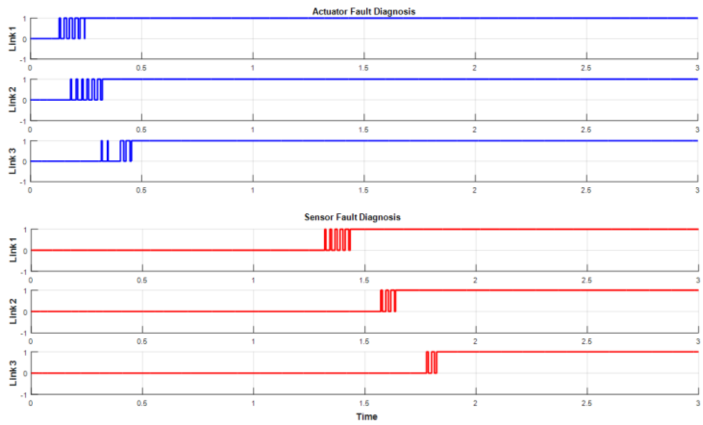

Fig. 9 Fault diagnosis in first three links of robot manipulator with actuator+sensor faulty condition

Table 1 Fault diagnosis delays for ARX-Laguerre PIO and ARX-PIO for first three links in normal condition

Links	Actuator diagnosis delay (s)		Sensor diagnosis delay (s)	
	ARX-Laguerre PIO	ARX-PIO	ARX-Laguerre PIO	ARX-PIO
1	0	0	0	0
2	0	0	0	0
3	0	0	0	0

Table 2 Fault diagnosis delays for ARX-Laguerre PIO and ARX-PIO for first three links in the presence of actuator fault

Links	Actuator diagnosis delay (s)		Sensor diagnosis delay (s)	
	ARX-Laguerre PIO	ARX-PIO	ARX-Laguerre PIO	ARX-PIO
1	0.14	0.17	0	0
2	0.1706	0.21	0	0
3	0.2385	0.34	0	0

Table 3 Fault diagnosis delays for ARX-Laguerre PIO and ARX-PIO for first three links in the presence of sensor fault

Links	Actuator diagnosis delay (s)		Sensor diagnosis delay (s)	
	ARX-Laguerre PIO	ARX-PIO	ARX-Laguerre PIO	ARX-PIO
1	0	0	0.166	0.265
2	0	0	0.322	0.514
3	0	0	0.504	0.792

Table 4 Fault diagnosis delays for ARX-Laguerre PIO and ARX-PIO for first three links in the presence of actuator+sensor faults

Links	Actuator diagnosis delay (s)		Sensor diagnosis delay (s)	
	ARX-Laguerre PIO	ARX-PIO	ARX-Laguerre PIO	ARX-PIO
1	0.1438	0.1921	0.442	0.678
2	0.2227	0.2563	0.638	0.695
3	0.3539	0.4143	0.822	0.91

Table 5 Fault diagnosis accuracy for first three links in normal condition (ARX-Laguerre PIO and ARX-PIO)

Links	Actuator diagnosis delay (s)		Sensor diagnosis delay (s)	
	ARX-Laguerre PIO	ARX-PIO	ARX-Laguerre PIO	ARX-PIO
1	100%	100%	100%	100%
2	100%	100%	100%	100%
3	100%	100%	100%	100%

Table 6 Fault diagnosis accuracy for first three links in in the presence of actuator fault (ARX-Laguerre PIO and ARX-PIO)

Links	Actuator diagnosis delay (s)		Sensor diagnosis delay (s)	
	ARX-Laguerre PIO	ARX-PIO	ARX-Laguerre PIO	ARX-PIO
1	99.53%	94.3%	100%	100%
2	94.13%	91%	100%	100%
3	92.05%	89%	100%	100%

Table 7 Fault diagnosis accuracy for first three links in in the presence of sensor fault (ARX-Laguerre PIO and ARX-PIO)

Links	Actuator diagnosis delay (s)		Sensor diagnosis delay (s)	
	ARX-Laguerre PIO	ARX-PIO	ARX-Laguerre PIO	ARX-PIO
1	100%	100%	94.47%	90.1%
2	100%	100%	89.3%	83.2%
3	100%	100%	87.2%	80%

Table 8 Fault diagnosis accuracy for first three links in in the presence of actuator+sensor faults (ARX-Laguerre PIO and ARX-PIO)

Links	Actuator diagnosis delay (s)		Sensor diagnosis delay (s)	
	ARX-Laguerre PIO	ARX-PIO	ARX-Laguerre PIO	ARX-PIO
1	95.2%	90%	88.3%	87.12%
2	92.58%	87.12%	82.1%	80%
3	90.5%	81.1%	80.1%	78.1%

As shown in Tables 5-8, the accuracy of fault detection and diagnosis in FFPGA-based ARX PI observer for normal condition, actuator faulty, sensor faulty, and composed faulty conditions are 100%, 91.4%, 84.43%, and 83.9%, and in proposed FPGA-based ARX-Laguerre PI observer for normal, actuator faulty, sensor faulty, and multi (actuator+sensor) defective condition is 100%, 97.7%, 95.16% and 88.13%, respectively. The accuracy performance result can be further validated by the fact that proposed FPGA-based ARX-Laguerre PI observer technique is highly sufficient to identify the signal state and define the dynamic error threshold, as can be seen in Figs. 6-9 and Tables 5-8.

6. Conclusions

In this paper, the proposed method for fault diagnosis in robot manipulators is analyzed. In the first step, robot manipulator was modeled in the presence of uncertainty and external disturbance based on the ARX method and proposed ARX-Laguerre dynamic modeling. The proposed technique is used for modeling and fault detection in the presence of actuator and sensor faults. To identification and estimation, the actuator and sensor faults, FPGA-based PI observation technique has been recommended. In this technique, the integral part is used to fault estimation, reduce the steady-state error and improve the stability. The effectiveness of proposed ARX-Laguerre PI observer technique is tested by PUMA robot manipulator, which outperforms the ARX- PI observer, yielding 6.3%, 10.73%, and 4.23%, average performance improvement for three types of faults (e.g., actuator fault, sensor faults, and composite fault), respectively.

Acknowledgements

This work was supported by the Korea Institute of Energy Technology Evaluation and Planning (KETEP) and the Ministry of Trade, Industry & Energy (MOTIE) of the Republic of Korea (No. 20162220100050, No. 20161120100350, and No. 20172510102130). It was also funded in part by the Leading Human Resource Training Program of Regional Neo Industry through the National Research Foundation of Korea (NRF) funded by the Ministry of Science, ICT and future Planning (NRF-2016H1D5A1910564), and in part by the Basic Science Research Program through the National Research Foundation of Korea (NRF) funded by the Ministry of Education (2016R1D1A3B03931927).

References

Alavandar, S. and Nigam, M.J. (2008), "Neuro-fuzzy based approach for inverse kinematics solution of industrial robot manipulators", *J. Comput. Commun. Contr.*, **3**(3), 224-234.

Alwi, H. and Edwards, C. (2014), "Robust fault reconstruction for linear parameter varying systems using sliding mode observers", *J. Robust Nonlin. Contr.*, **24**(14), 1947-1968.

Anh, H.P.H. and Nam, N.T. (2012), "Novel adaptive forward neural MIMO NARX model for the identification of industrial 3-DOF robot arm kinematics", *J. Adv. Robot. Syst.*, **9**(4), 104.

Badihi, H., Zhang, Y. and Hong, H. (2017), "Fault-tolerant cooperative control in an offshore wind farm using model-free and model-based fault detection and diagnosis approaches", *Appl. Energy*, **201**, 284-307.

Bouzrara, K., Garna, T., Ragot, J. and Messaoud, H. (2013), "Online identification of the ARX model expansion on Laguerre orthonormal bases with filters on model input and output", *J. Contr.*, **86**(3), 369-385.

Bouzrara, K., Garna, T., Ragot, J. and Messaoud, H. (2012), "Decomposition of an ARX model on Laguerre orthonormal bases", *ISA Trans.*, **51**(6), 848-860.

Busawon, K.K. and Kabore, P. (2001), "Disturbance attenuation using proportional integral observers", *J. Contr.*, **74**(6), 618-627.

Forrai, A. (2017), "System identification and fault diagnosis of an electromagnetic actuator", *IEEE T. Contr. Syst. Technol.*, **25**(3), 1028-1035.

Gao, Z., Breikin, T. and Wang, H. (2008), "Discrete-time proportional and integral observer and observer-based controller for systems with both unknown input and output disturbances", *Optim. Contr. Appl. Met.*, **29**(3), 171-189.

Gao, Z. and Ho, D.W. (2004), "Proportional multiple-integral observer design for descriptor systems with measurement output disturbances", *IEE Proc. Contr. Theor. Appl.*, **151**(3), 279-288.

Gao, Z., Ding, S.X. and Ma, Y. (2007), "Robust fault estimation approach and its application in vehicle lateral dynamic systems", *Optim. Contr. Appl. Met.*, **28**(3), 143-156.

Gao, Z. and Wang, H. (2006), "Descriptor observer approaches for multivariable systems with measurement noises and application in fault detection and diagnosis", *Syst. Control Lett.*, **55**(4), 304-313.

Gao, Z., Shi, X. and Ding, S.X. (2008), "Fuzzy state/disturbance observer design for T-S fuzzy systems with application to sensor fault estimation", *IEEE T. Syst. Man. Cy. B*, **38**(3), 875-880.

Gao, Z., Dai, X., Breikin, T. and Wang, H. (2008), "Novel parameter identification by using a high-gain observer with application to a gas turbine engine", *IEEE T. Ind. Inform.*, **4**(4), 271-279.

Gholizadeh, M. and Salmasi, F.R. (2014), "Estimation of state of charge, unknown nonlinearities, and state of health of a lithium-ion battery based on a comprehensive unobservable model", *IEEE T. Ind. Electron.*, **61**(3), 1335-1344.

Han, X., Fridman, E. and Spurgeon, S.K. (2014), "Sampled-data sliding mode observer for robust fault reconstruction: A time-delay approach", *J. Franklin Inst.*, **351**(4), 2125-2142.

Hartmann, A., Lemos, J.M., Costa, R.S., Xavier, J. and Vinga, S. (2015), "Identification of switched ARX models via convex optimization and expectation maximization", *J. Process Contr.*, **28**, 9-16.

Jami'in, M.A., Hu, J., Marhaban, M.H., Sutrisno, I. and Mariun, N.B. (2016), "Quasi-ARX neural network based adaptive predictive control for nonlinear systems", *IEEJ Trans. Elect. Electron. Eng.*, **11**(1), 83-90.

Jamshidpour, E., Poure, P. and Saadate, S. (2015), "Photovoltaic systems reliability improvement by real-time FPGA-based switch failure diagnosis and fault-tolerant DC-DC converter", *IEEE T. Ind. Electron.*, **62**(11), 7247-7255.

Kang, M., Kim, J. and Kim, J.M. (2015), "An FPGA-based multicore system for real-time bearing fault diagnosis using ultrasampling rate AE signals" *IEEE T. Ind. Electron.*, **62**(4), 2319-2329.

Khalastchi, E., Kalech, M. and Rokach, L. (2017), "A hybrid approach for improving unsupervised fault detection for robotic systems", *Expert Syst. Appl.*, **81**, 372-383.

Koenig, D. (2005), "Unknown input proportional multiple-integral observer design for linear descriptor systems: Application to state and fault estimation", *IEEE T. Autom. Contr.*, **50**(2), 212-217.

Lafont, F., Balmat, J.F., Pessel, N. and Fliess, M. (2015), "A model-free control strategy for an experimental greenhouse with an application to fault accommodation", *Comput. Electron. Agr.*, **110**, 139-149.

López-Estrada, F.R., Ponsart, J.C., Theilliol, D., Zhang, Y. and Astorga-Zaragoza, C.M. (2016), "LPV model-based tracking control and robust sensor fault diagnosis for a quadrotor UAV", *J. Intell. Robot. Syst.*, **84**(1-4), 163-177.

Ngoc Son, N., Anh, H.P.H. and Thanh Nam, N. (2016), "Robot manipulator identification based on adaptive multiple-input and multiple-output neural model optimized by advanced differential evolution algorithm", *J. Adv. Robot. Syst.*, **14**(1), 1729881416677695.

Salehifar, M., Arashloo, R.S., Eguilaz, M.M. and Sala, V. (2015), "FPGA based robust open transistor fault diagnosis and fault tolerant sliding mode control of five-phase PM motor drives", *J. Power Electron.*, **15**(1), 131-145.

Siciliano, B. and Khatib, O. (2016), *Springer Handbook of Robotics*, Springer.

Simani, S., Fantuzzi, C. and Patton, R.J. (2013), *Model-Based Fault Diagnosis in Dynamic Systems Using Identification Techniques*, Springer Science & Business Media.

Stavrou, D., Eliades, D.G., Panayiotou, C.G. and Polycarpou, M.M. (2016), "Fault detection for service mobile robots using model-based method", *Autonom. Robot.*, **40**(2), 383-394.

Van, M., Franciosa, P. and Ceglarek, D. (2016), "Fault diagnosis and fault-tolerant control of uncertain robot manipulators using high-order sliding mode", *Math. Probl. Eng.*

Wang, X., Li, X., Wang, J., Fang, X. and Zhu, X. (2016), "Data-driven model-free adaptive sliding mode control for the multi degree-of-freedom robotic exoskeleton", *Inform. Sci.*, **327**, 246-257.

Xia, X., Zhou, J., Xiao, J. and Xiao, H. (2016), "A novel identification method of Volterra series in rotor-bearing system for fault diagnosis", *Mech. Syst. Signal Pr.*, **66**, 557-567.

Zhang, K., Jiang, B., Cocquempot, V. and Zhang, H. (2013), "A framework of robust fault estimation observer design for continuous-time/discrete-time systems", *Optim. Contr. Appl. Met.*, **34**(4), 442-457.

Zhang, Q. and Besancon, G. (2008), "An adaptive observer for sensor fault estimation in a class of uniformly observable non-linear systems", *J. Modell. Identific. Contr.*, **4**(1), 37-43.

Zhang, K., Jiang, B. and Cocquempot, V. (2008), "Adaptive observer-based fast fault estimation", *J. Contr. Autom. Syst.*, **6**(3), 320-326.

Zhang, J., Swain, A.K. and Nguang, S.K. (2013), "Robust sensor fault estimation scheme for satellite attitude control systems", *J. Franklin Inst.*, **350**(9), 2581-2604.

HM